the presence of an overlapping and intensely absorbing MLCT band in the $W(CO)_5$(4-CNpy) complex is also an important factor in reducing the efficiency of LF population and, hence, ^{3}LF photochemistry.

Acknowledgment. We gratefully acknowledge the donors of the Petroleum Research Fund, administered by the American Chemical Society, for support of this research. We also thank Mr. Zhikai Wang for assistance with the lifetime measurements.

Contribution from the Laboratoire de Chimie Théorique, Université de Paris-Sud, 91405 Orsay, France, and Department of Chemistry, North Carolina State University, Raleigh, North Carolina 27695-8204

Similarity of the Electronic Properties of the Monophosphate Tungsten Bronzes

Enric Canadell,*[†] Myung-Hwan Whangbo,*[‡] and Idris El-Idrissi Rachidi[†]

Received January 17, 1990

The electronic structures of the perovskite-type tungsten oxide (W–O) layers of the monophosphate tungsten bronzes (MPTB) were examined by performing tight-binding band calculations. Our study shows that all known MPTB phases have one- and two-dimensional metallic bands regardless of the difference in the thickness of their W–O layers and in their octahedral distortions. Concerning this dimensionality of the electronic properties, the bond valence sum analysis is found to give erroneous predictions. We examine the origin of this failure and also that of the remarkable similarity in the MPTB electronic structures.

The monophosphate tungsten bronzes (MPTB) contain perovskite-type layers made up of WO_6 octahedra, and these tungsten oxide (W–O) layers are interlinked by PO_4 tetrahedra.[1,2] The thickness of these W–O layers increase with the number of WO_6 octahedra (per unit cell) used to form the layers. The MPTB phases have either pentagonal or hexagonal tunnels between the W–O layers, and they are called the $MPTB_p$ and $MPTB_h$ phases, respectively. The latter invariably occur with alkali-metal atoms Na or K, which reside in the hexagonal tunnels.[2] The third members of the $MPTB_p$ and $MPTB_h$ series, $(WO_3)_6(WO_3)_6(PO_2)_4$ and $A_x(WO_3)_6(WO_3)_6(PO_2)_4$ (A = alkali metal), are similar in structure to the Magnéli phases[3] γ-Mo_4O_{11} and η-Mo_4O_{11}, respectively, except that PO_4 tetrahedra are replaced by MoO_4 tetrahedra in the Magnéli phases. The latter exhibit resistivity anomalies,[4] which originate from the electronic instability associated with the partially filled bands of their perovskite-type Mo–O layers.[5] Since the MPTB phases possess isostructural W–O layers, they are also expected to show similar electronic instabilities. In fact, the third member of the $MPTB_p$ series, $(WO_3)_6(WO_3)_6(PO_2)_4$, exhibits resistivity anomalies[6] strikingly similar to those of $NbSe_3$, a well-established charge-density-wave (CDW) material.[7]

As will be discussed later, each perovskite-type W–O layer of the $MPTB_p$ series contains two d electrons per unit cell, regardless of its thickness. This electron counting is slightly modified in the $MPTB_h$ phases due to the alkali-metal atoms in their hexagonal channels. Thus, the MPTB phases provide a number of W–O layers with different average oxidation states of W. The crystal structures of the MPTB series reveal that the octahedral distortions in their W–O layers are not uniform even among those layers with a same thickness. In understanding the electronic properties of the MPTB phases, it is necessary to examine how their electronic structures are related to the crystal structure, the octahedral distortion, and the average oxidation state of W. In the present study, we investigate the electronic structures of all MPTB phases with known crystal structures by performing tight-binding band calculations[8] based upon the extended Hückel method.[9] The atomic parameters employed in the present study are taken from our previous work.[10]

Crystal Structure

Nearly all MPTB phases have two perovskite-type W–O layers per unit cell.[1,2] Thus, the general formulas for the $MPTB_p$ phases can be written as $(WO_3)_p(WO_3)_q(PO_2)_4$, and those for the $MPTB_h$ phases as $A_x(WO_3)_p(WO_3)_q(PO_2)_4$ (A = Na, K). The indices p and q are even or odd integers, which are equal to the number of WO_6 octahedra (per unit cell) used to form the W–O layer. Usually p and q are identical, thereby leading to the formulas $(WO_3)_{2m}(PO_2)_4$ and $A_x(WO_3)_{2m}(PO_2)_4$ (m = integer). However, they can be different as in the case of $(WO_3)_4(WO_3)_6(PO_2)_4$, which should be distinguished from $(WO_3)_5(WO_3)_5(PO_2)_4$.

The general structural patterns of the perovskite-type W–O layers may be described in terms of the W–O layer with $p = 4$. Diagram **1** shows a perspective view of the W_4O_{21} unit made up

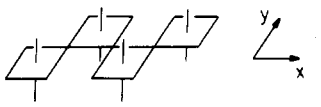

1

[†] Université de Paris-Sud.
[‡] North Carolina State University.

(1) (a) Giroult, J. P.; Goreaud, M.; Labbé, P.; Raveau, B. *Acta Crystallogr. Sect. B* **1981**, *B37*, 2139. (b) Labbé, P.; Goreaud, M.; Raveau, B. *J. Solid State Chem.* **1986**, *61*, 324. (c) Benmoussa, A.; Labbé, P.; Giroult, D.; Raveau, B. *J. Solid State Chem.* **1982**, *44*, 318. (d) Domengès, B.; Studer, F.; Raveau, B. *Mater. Res. Bull.* **1983**, *18*, 669. (e) Domengès, B.; Hervieu, M.; Raveau, B.; Tilley, R. J. D. *J. Solid State Chem.* **1984**, *54*, 10.
(2) (a) Giroult, J. P.; Goreaud, M.; Labbé, P.; Raveau, B. *J. Solid State Chem.* **1982**, *44*, 407. (b) Benmoussa, A.; Giroult, D.; Labbé, P.; Raveau, B. *Acta Crystallogr., Sect. C* **1984**, *C40*, 573. (c) Domengès, B.; Goreaud, M.; Labbé, P.; Raveau, B. *J. Solid State Chem.* **1983**, *50*, 173. (d) Lamire, M.; Labbé, P.; Goreaud, M.; Raveau, B. *J. Solid State Chem.* **1987**, *66*, 64. (e) Benmoussa, A.; Giroult, D.; Raveau, B. *Rev. Chim. Min.* **1984**, *21*, 710.
(3) (a) Ghedira, M.; Vincent, H.; Marezio, M.; Marcus, J.; Fourcadot, G. *J. Solid State Chem.* **1985**, *56*, 66. (b) Kihlborg, L. *Arkiv Kemi* **1963**, *21*, 365. (c) Magnéli, A *Acta Chem. Scand.* **1948**, *2*, 861.
(4) (a) Guyot, H.; Schlenker, C.; Fourcadot, G.; Konaté, K. *Solid State Commun.* **1985**, *54*, 909. (b) Sato, M.; Nakao, K.; Hoshino, S. *J. Phys. C* **1984**, *17*, L817. (c) Schlenker, C.; Parkin, S. S. P.; Guyot, H. *J. Magn. Magn. Mater.* **1986**, *54–57*, 1313. (d) Guyot, H.; Escribe-Filippini, C.; Fourcadot, G.; Konaté, K.; Schlenker, C. *J. Phys. C* **1983**, *16*, L1227.
(5) Canadell, E.; Whangbo, M.-H.; Schlenker, C.; Escribe-Filippini, C. *Inorg. Chem.* **1989**, *28*, 1466.
(6) Wang, E.; Greenblatt, M.; Rachidi, I. E.-I.; Canadell, E.; Whangbo, M.-H.; Vadlamannati, S. *Phys. Rev. B.* **1989**, *39*, 12969.
(7) (a) Monceau, P. In *Electronic Properties of Inorganic Quasi-One-Dimensional Compounds. Part II.* Monceau, P., Ed.; Reidel: Dordrecht, The Netherlands, 1985; p 139. (b) Haen, P.; Monceau, P.; Tissier, B.; Waysand, G.; Meerschaut, A.; Molinié, P.; Rouxel, J. In *Proceedings of the Fourteenth International Conference on Low Temperature Physics*; Krusius, M., Vuorio, M., Eds.; North Holland: New York, 1975. (c) Canadell, E.; Rachidi, I. E.-I.; Pouget, J. P.; Gressier, P.; Meerschaut, A.; Rouxel, J.; Jung, D.; Evain, M.; Whangbo, M.-H. *Inorg. Chem.* **1990**, *29*, 1401.
(8) Whangbo, M.-H.; Hoffmann, R. *J. Am. Chem. Soc.* **1978**, *100*, 6093.
(9) Hoffmann, R. *J. Chem. Phys.* **1963**, *39*, 1397. A modified Wolfsberg–Helmholz formula was used to calculate the off-diagonal H_{ij} values. See: Ammeter, J. H.; Burgi, H.-B.; Thibeault, J.; Hoffmann, R. *J. Am. Chem. Soc.* **1978**, *100*, 2686.
(10) Wang, E.; Greenblatt, M.; Rachidi, I. E.-I.; Canadell, E.; Whangbo, M.-H. *Inorg. Chem.* **1989**, *28*, 2451.

0020-1669/90/1329-3871$02.50/0

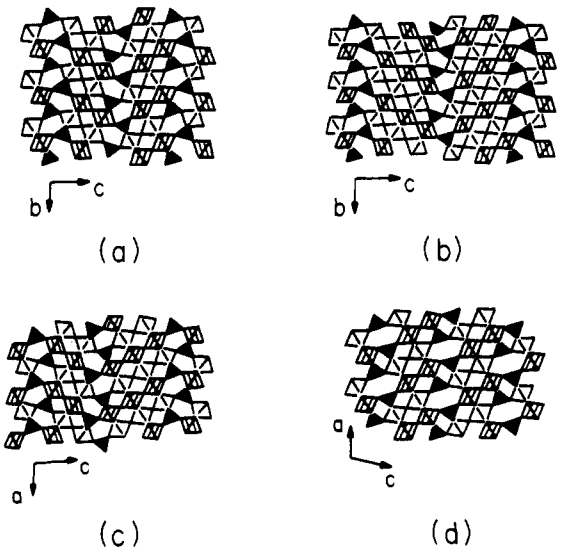

Figure 1. Projection view of representative MPTB phases: (a) $(WO_3)_4(WO_3)_4(PO_2)_4$;[1a] (b) $(WO_3)_6(WO_3)_6(PO_2)_4$;[1b] (c) $(WO_3)_4(WO_3)_6(PO_2)_4$;[1c] (d) $Na_x(WO_3)_4(WO_3)_4(PO_2)_4$.[2b]

of four WO_6 octahedra by sharing corners. These W_4O_{21} units may be condensed to form a W_4O_{18} chain **2a**, which can be

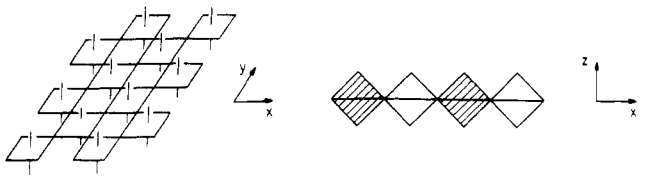

2a **2b**

represented by a projection view **2b** along the chain direction. Finally, the W_4O_{18} chains can be condensed to form a W_4O_{16} layer **3a**, in which the first octahedron of one W_4O_{18} chain (in the

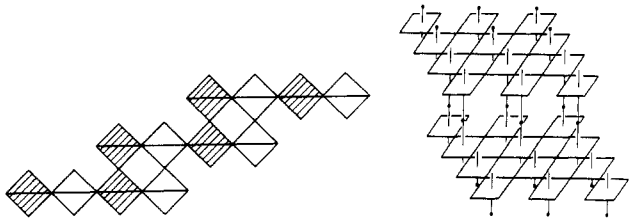

3a **3b**

projection view **2b**) shares its axial oxygen atom with the third octahedron of the adjacent W_4O_{18} chain [i.e., (13)-condensation]. A perspective view of **3a** is given by **3b**, which shows that it is a step layer with each W_4O_{18} chain as a step. Likewise, one can condense the W_6O_{31} units (**4**) to construct a W_6O_{26} chain **5**, and

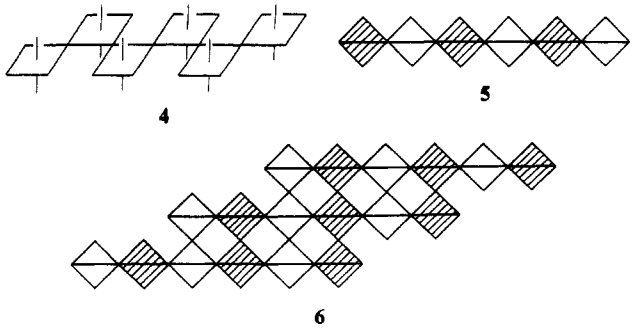

4 **5**

6

the W_6O_{22} layer **6** is obtained by the (13)-condensation of the W_6O_{26} chains **5**. The structural patterns of the Mo_6O_{22} layers of the Magnéli phases γ-Mo_4O_{11} and η-Mo_4O_{11}[3] are identical with those of the W_6O_{22} layer shown in **6**. Figure 1 shows projection views of four representative MPTB phases, $(WO_3)_4(WO_3)_4(PO_2)_4$, $(WO_3)_6(WO_3)_6(PO_2)_4$, $(WO_3)_4(WO_3)_6(PO_2)_4$, and $Na_x(WO_3)_4(WO_3)_4(PO_2)_4$, where the filled triangles refer to the PO_4 tetrahedra.

Table I. Oxidation States of the W_I and W_{II} Atoms in the W_4O_{16} Layers Calculated by the Bond Valence Sum Rule

compd	oxidn state	
	W_I	W_{II}
$(WO_3)_4(WO_3)_4(PO_2)_4$	5.82	5.18
$(WO_3)_4(WO_3)_6(PO_2)_4$	5.28	5.82
$Na_{1.5}(WO_3)_4(WO_3)_4(PO_2)_4$	5.24	5.38

Dimensionality of the Electronic Properties Predicted by the Bond Valence Sum Analysis

For complex oxide metals with large unit cells but with a few d electrons per unit cell (e.g., the MPTB phases and molybdenum oxides[11]), it is important to know which portions of the crystals contain the d electrons and hence are largely responsible for their electrical conductivities. Empirically, this question has been answered by the bond valence sum analysis,[12] which allows one to estimate the oxidation state of a metal on the basis of the metal–oxygen bond lengths it makes with the surrounding oxygen atoms. For example, the bond valence sum analyses on $K_{0.9}Mo_6O_{17}$,[13] $Li_{0.9}Mo_6O_{17}$,[14] Mo_4O_{11},[3a] and $K_{0.3}MoO_3$[15] predict that only certain MoO_6 octahedra of their Mo–O layers can have d electrons, in good agreement with the band electronic structure calculations.[5,11,16] In addition, the analysis for $Li_{0.9}Mo_6O_{17}$[14] shows that the d-electron containing MoO_6 octahedra form chains separated by the MoO_6 octahedra without d electrons. Consequently, $Li_{0.9}Mo_6O_{17}$ is predicted[14] to be a one-dimensional (1D) metal despite its three-dimensional (3D) crystal lattice. This prediction is in good agreement with the band electronic structure calculations[16b] and the experiment.[14]

Thus, it is of interest to perform the bond valence sum analysis for the MPTB phases. The parameters needed for this analysis have been developed by Domengès et al.[17] We note that there are two nonequivalent W atoms (W_I and W_{II}) in the W_4O_{16} layers of $(WO_3)_4(WO_3)_4(PO_2)_4$, $(WO_3)_4(WO_3)_6(PO_2)_4$, and $Na_x(WO_3)_4(WO_3)_4(PO_2)_4$ ($x = 1.5$) of Figure 1. Every W_IO_6 octahedron shares five oxygen atoms with other WO_6 octahedra and one oxygen atom with a PO_4 tetrahedra, while every $W_{II}O_6$ octahedron shares three oxygen atoms with other WO_6 octahedra and three oxygen atoms with PO_4 tetrahedra. Table I summarizes the oxidation states of the W_I and W_{II} atoms calculated for the three different W_4O_{16} layers by the bond valence sum analysis. For $Li_{0.9}Mo_6O_{17}$ and Mo_4O_{11}, it is reasonable to consider that the Mo atoms with oxidation state +5.7 or greater do not contain d electrons and those with oxidation state +5.4 or smaller have d electrons. According to this approximation, the d-electron-containing WO_6 octahedra are isolated in the W_4O_{16} layer of $(WO_3)_4(WO_3)_4(PO_2)_4$ (shaded octahedra in Figure 2a) but form a continuous chain in the W_4O_{16} layer of $(WO_3)_4(WO_3)_6(PO_2)_4$ (shaded octahedra in Figure 2b). On the other hand, all WO_6 octahedra are expected to have d electrons in the W_4O_{16} layer of $Na_x(WO_3)_4(WO_3)_4(PO_2)_4$ ($x = 1.5$) (Figure 2c). Therefore,

(11) Whangbo, M.-H.; Canadell, E. *Acc. Chem. Res.* **1989**, *22*, 375.
(12) (a) Zachariasen, W. H. *J. Less-Common Met.* **1978**, *62*, 1. (b) Brown, I. D. In *Structure and Bonding in Crystals*; O'Keeffe, M., Navrotsky, A., Eds.; Academic Press: New York, 1981; Vol. II, pp 1–30. (c) O'Keeffe, M. *Struct. Bonding* **1989**, *71*, 161.
(13) Vincent, H.; Ghedira, M.; Marcus, J.; Mercier, J.; Schlenker, C. *J. Solid State Chem.* **1983**, *43*, 113.
(14) Onoda, M.; Toriumi, K.; Matsuda, Y.; Sato, M. *J. Solid State Chem.* **1987**, *66*, 163.
(15) Ghedira, M.; Chenavas, J.; Marezio, M.; Marcus, J. *J. Solid State Chem.* **1985**, *57*, 300.
(16) (a) Whangbo, M.-H.; Canadell, E.; Schlenker, C. *J. Am. Chem. Soc.* **1987**, *109*, 6308. (b) Whangbo, M.-H.; Canadell, E. *J. Am. Chem. Soc.* **1988**, *110*, 358. (c) Whangbo, M.-H.; Schneemeyer, L. F. *Inorg. Chem.* **1986**, *25*, 2424.
(17) Domengès, B.; McGuire, N. K.; O'Keeffe, M. *J. Solid State Chem.* **1985**, *56*, 94.

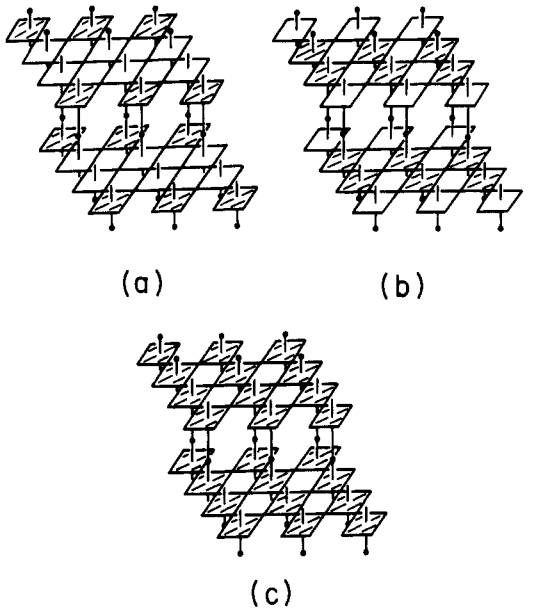

Figure 2. Perspective views of the W_4O_{16} layers found in (a) $(WO_3)_4(WO_3)_4(PO_2)_4$, (b) $(WO_3)_4(WO_3)_6(PO_2)_4$, and (c) $Na_{1.5}(WO_3)_4(WO_3)_4(PO_2)_4$. The shaded octahedra are predicted to contain d electrons by the bond valence sum analysis.

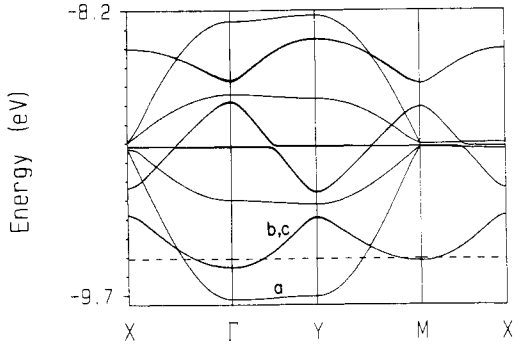

Figure 3. Dispersion relations of the t_{2g}-block bands calculated for an ideal W_4O_{16} layer (dashed line refers to the Fermi level corresponding to 2 d electrons per unit cell). $\Gamma = (0, 0)$, $X, = (a^*/2, 0)$, $Y = (0, b^*/2)$, and $M = (a^*/2, b^*/2)$, where a and b refer to the intra- and interchain directions, respectively.

Figure 2 suggests that the W_4O_{16} layers are nonmetallic in $(WO_3)_4(WO_3)_4(PO_2)_4$, are 1D metallic in $(WO_3)_4(WO_3)_6(PO_2)_4$, and are two-dimensional (2D) metallic in $Na_{1.5}(WO_3)_4(WO_3)_4(PO_2)_4$.

Band Electronic Structure

A. Ideal W_4O_{16} Layer. For the purpose of d-electron counting, the general formula of the MPTB phases may be written as $A_x(WO_3)_p(WO_3)_q(PO_2)_4$. With the formal oxidation states of A^+, P^{5+}, and O^{2-}, the average oxidation state of W is given by $6 - (4 + x)/(p + q)$. Thus, a unit cell of an MPTB phase has $4 + x$ electrons or, equivalently, $2 + x/2$ electrons per W–O layer. Namely, there exist $2 + x/2$ electrons per unit cell to fill the t_{2g}-block bands of a W–O layer.

Figure 3 shows the dispersion relations of the t_{2g}-block bands calculated for an ideal W_4O^{16} layer made up of regular WO_6 octahedra (with the average W–O distance of 1.916 Å), where the dashed line refers to the Fermi level appropriate for 2 electrons per unit cell. These t_{2g}-block bands are essentially identical in nature with those of an ideal Mo_4O_{16} layer examined in connection with the Mo_4O_{11} electronic structure.[5] The Fermi level of Figure 3 cuts the 1D band (i.e., band a) as well as the two nearly degenerate 2D bands (i.e., bands b and c). This result is obtained because bands b,c occur in the middle of band a. For the same reason, the Fermi level for any d-electron count between 2 and 4 per unit cell would make all bands a–c partially filled.

A band orbital analysis for why bands b,c occur in the middle of band a is discussed in detail elsewhere.[5] For our discussions that follow, we need to mention only briefly why, at Γ, the bottoms of bands b,c are close in energy to that of band a. An ideal WO_6 octahedron has three t_{2g}-block levels shown in **7**. At Γ, bands

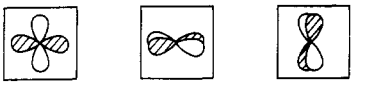

7

a–c of the W_4O_{16} layer have no p-orbital contributions from the shared oxygen atoms both within and between the W_4O_{18} chains (i.e., the steps of the W_4O_{16} layers). This can be shown in terms of the band orbitals of the W_4O_{18} chain: Shown in **8** is the orbital

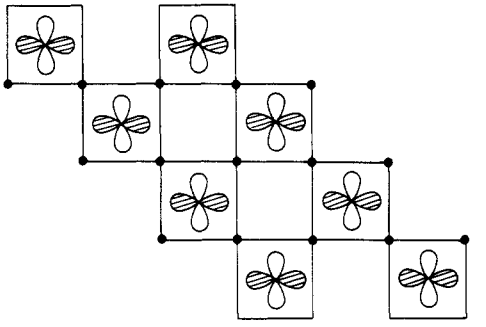

8

for band a, which is constructed from the δ orbital (i.e., x^2-y^2 in **7**) of WO_6 octahedra. **9** and **10** are the orbitals for bands b and

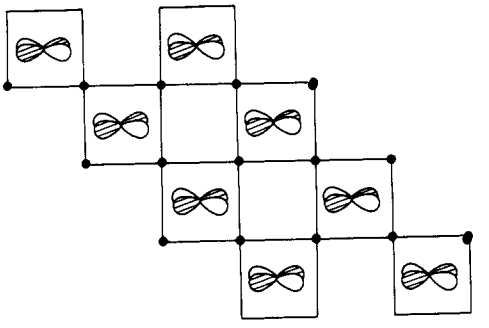

9

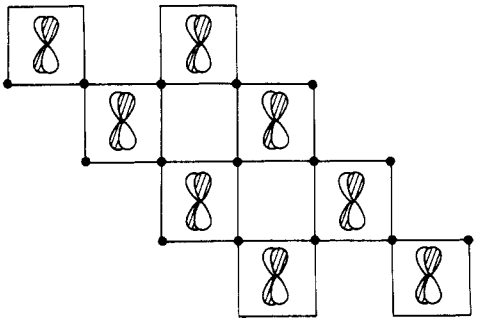

10

c, respectively, which are constructed from the π orbitals (i.e., xz and yz in **7**). Since at Γ the shared oxygen atoms do not contribute their p orbitals to mix with the metal d orbitals, the band orbitals **9** and **10** are close in energy to **8**. The bottoms of bands b,c are somewhat higher in energy than that of band a, due to the difference in the p-orbital contributions from the unshared oxygen atoms

B. Real W_4O_{16} Layers. The dispersion relations of the bottom portions of the t_{2g}-block bands calculated for the W_4O_{16} layers in $(WO_3)_4(WO_3)_4(PO_2)_4$, $(WO_3)_4(WO_3)_6(PO_2)_4$, and $Na_x(WO_3)_4(WO_3)_4(PO_2)_4$ (x = 1.1–1.5) are shown in Figure 4a–c, respectively. All these bands are very similar to those of the ideal

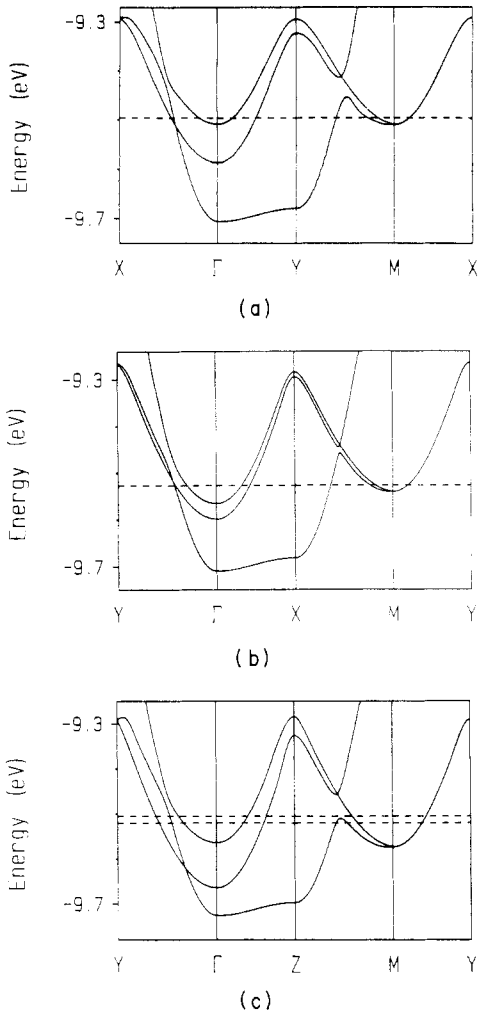

Figure 4. Dispersion relations of the bottom portions of the t_{2g}-block bands calculated for the W_4O_{16} layers of (a) $(WO_3)_4(WO_3)_4(PO_2)_4$, (b) $(WO_3)_4(WO_3)_6(PO_2)_4$, and (c) $Na_x(WO_3)_4(WO_3)_4(PO_2)_4$. $\Gamma = (0, 0)$, $X = (a^*/2, 0)$, $Y = (0, b^*/2)$, and $M = (a^*/2, b^*/2)$. The chain direction is given along $\Gamma \rightarrow X$ in (a) but along $\Gamma \rightarrow Y$ in (b) and (c). The dashed lines in (a) and (b) refer to the Fermi level corresponding to 2 d electrons per unit cell. In (c) the two dashed lines refer to the Fermi levels appropriate for 2.55 and 2.75 d electrons per unit cell (i.e., $x = 1.1$ and 1.5), respectively.

W_4O_{16} layer shown in Figure 3, except that bands b,c are split in the real W_4O_{16} layers because of their octahedral distortions. The most important aspect of Figure 4 is that the W_4O_{16} layers of $(WO_3)_4(WO_3)_4(PO_2)_4$ and $(WO_3)_4(WO_3)_6(PO_2)_4$ have both 1D and 2D metallic bands, as does that of $Na_x(WO_3)_4(WO_3)_4(PO_2)_4$. This is in sharp contrast to the prediction of the bond valence sum analysis discussed in the previous section. This failure of the bond valence sum analysis is striking, in view of its general success in the molybdenum oxide metals. The major reason for this failure is that the orbitals of bands a–c in the W_4O_{16} layers of $(WO_3)_4(WO_3)_4(PO_2)_4$ and $(WO_3)_4(WO_3)_6(PO_2)_4$ have nearly equal contributions from their W_I and W_{II} atoms, just as in the case of the corresponding bands in $Na_x(WO_3)_4(WO_3)_4(PO_2)_4$. In the following, we examine why this is the case.

C. Octahedral Distortion and Bond Valence Sum Analysis. A series of electronic structure studies on the molybdenum oxide metals have shown[11,18] that their lowest lying d-block bands are determined by the nature of the octahedral distortions. A regular MoO_6 octahedron may be distorted to give one short Mo–O bond (**11** → **12a**) or more than one short Mo–O bond (**11** → **12b**). These distortions lead to the t_{2g}-level splitting shown in **13a** and

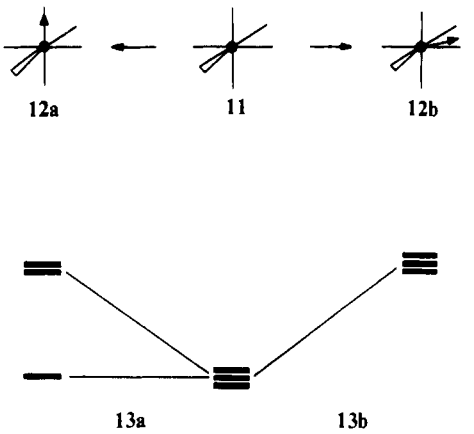

13b, respectively. Thus, for a perovskite-type Mo–O layer consisting of MoO_6 octahedra **12a** and **12b**, the lowest lying t_{2g}-block bands are represented by the lowest lying t_{2g}-block level of every MoO_6 octahedron **12a**.[11,18] In Mo_4O_{11} all MoO_6 octahedral have a distortion of type (**11** → **12b**). Of the three nonequivalent octahedra in the Mo_6O_{22} layer (**6**) of Mo_4O_{11}, one has a much stronger distortion than do the remaining two and therefore has high-lying t_{2g} orbitals. When those MoO_6 octahedra with high-lying t_{2g} levels (i.e., the end two MoO_6 octahedra of the Mo_6O_{26} step **5**) are removed, the Mo_6O_{22} layer **6** is simplified to become the Mo_4O_{16} layer **3**.[3a,5] That is, only the Mo_4O_{16} layer portion of the Mo_6O_{22} layer is expected to have d electrons. This orbital analysis is in agreement with the prediction of the bond valence sum analysis. The key point to note is that, of the three nonequivalent MoO_6 octahedra, one has a much stronger distortion than do the remaining two. The existence of such a large difference in the extents of octahedral distortion is necessary for the prediction of the bond valence sum analysis to agree with that of band electronic structure calculations. This is not the case for the MPTB phases. In the case of the Magnéli phase Mo_8O_{23}[19] as well, the bond valence sum analysis fails[20] to predict the correct dimensionality of the Mo_8O_{23} electronic properties for similar reasons.

D. Common Features of the Electronic Structures of the Perovskite-Type W–O Layers. In the ideal W_4O_{16} layer, the bottoms of bands b,c are close in energy to that of band a (Figure 3) because, at Γ, their symmetric metal–oxygen–metal (M–O–M) bridges do not allow the p-orbital contributions from the bridging oxygen atoms when the adjacent two metal orbitals have a same sign (see **14a**). If there were a strong M–O···M bond alternations

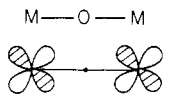

14a

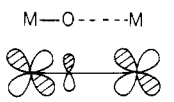

14b

(as consequence of octahedral distortion), the bridging oxygen p orbital combines out-of-phase with the metal d orbital of the shorter M–O bond even if the adjacent two metal orbitals have the same sign (see **14b**). Such an antibonding interaction raises the energy of **14b** with respect to **14a**. In the case of the MPTB phases, the W–O···W alternations are weak so that the bonding pattern of their W–O···W bridges at Γ is similar to that of **14a**. Thus, in the t_{2g}-block bands of the W_4O_{16} layers (Figure 4), the bottoms of bands a–c are represented by the W_I and W_{II} atoms

(18) (a) Canadell, E.; Whangbo, M.-H. *Inorg. Chem.* **1988**, *27*, 228. (b) Whangbo, M.-H.; Evain, M.; Canadell, E.; Ganne, M. *Inorg. Chem.* **1989**, *28*, 267.

(19) (a) Fujishita, H.; Sato, M.; Sato, S.; Hoshino, S. *J. Solid State Chem.* **1987**, *66*, 40. (b) Onoda, M.; Fujishita, H.; Matsuda, Y.; Sato, M. *Synth. Met.* **1987**, *19*, 947.

(20) Canadell, E.; Whangbo, M.-H. *Inorg. Chem.* **1990**, *29*, 2256.

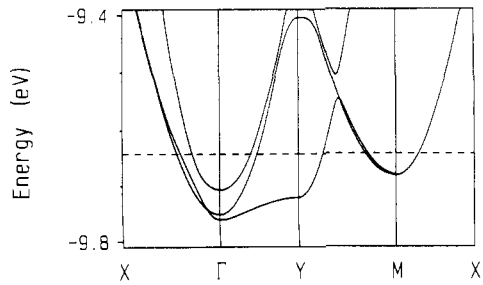

Figure 5. Dispersion relations of the bottom portion of the t_{2g}-block band calculated for the W_6O_{22} layer of $(WO_3)_6(WO_3)_6(PO_2)_4$. The dashed line refers to the Fermi level corresponding to 2 d electrons per unit cell.

almost equally. Lack of strong bridging p-orbital contributions also makes those three bands close in energy at Γ (from the viewpoint of the overall t_{2g}-block band dispersions).

In the perovskite-type W-O layers, the W atoms interact via the W-O-W bridges. Thus, a d-block band orbital in which contributions of the bridging oxygen p orbitals are absent would have an energy close to that of the atomic d level. This should be the case regardless of how many WO_6 octahedra per unit cell are used to form a perovskite-type W-O layer. For example, band a of the W_4O_{16} layer is constructed from the orbital pattern **15** (in each W_4O_{18} step **2**). Likewise, the corresponding band of the W_6O_{22} layer is constructed from the orbital pattern **16** (in each W_6O_{26} step **5**). Since **15** and **16** have similar energies and similar nodal patterns, the resulting bands a of the W_4O_{16} and W_6O_{22} layers should be similar. According to the same reasoning, it is predicted that the bottom three t_{2g}-block bands of the W_4O_{16} layer should be similar to those of the W_6O_{22} layer or any other perovskite-type W-O step layer. Since the W-O step layer of the MPTB phases have between 2 and 4 d electrons per unit cell, it is also predicted that all MPTB phases should have both 1D and

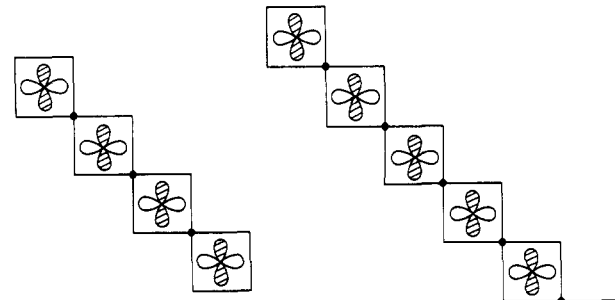

15

16

2D metallic bands. We have confirmed these predictions for all MPTB phases with known crystal structures. As a representative example, we show in Figure 5 the dispersion relations of the t_{2g}-block bands calculated for the W_6O_{22} step layer in $(WO_3)_6(WO_3)_6(PO_2)_4$.

Concluding Remarks

Our study shows that all MPTB phases should have both 1D and 2D metallic bands, regardless of the difference in their W-O layer thickness. This remarkable similarity originates from the fact that the W-O layers of the MPTB have between 2 and 4 d electrons per unit cell, and thus, only the bottom three of the t_{2g}-block bands can be partially filled due to their overlapping. Our sudy also shows that predictions of a bond valence sum analysis can be erroneous when the extents of metal-oxygen···metal bond alternations do not have a wide variation, as in the case of the MPTB phases.

Acknowledgment. This work was supported by the U.S. Department of Energy, Office of Basic energy Sciences, Division of Materials Sciences, under Grant DE-FG05-86ER45259.

Contribution from the Institut de chimie minérale et analytique, Université de Lausanne, 3, Place du Château, CH-1005 Lausanne, Switzerland

Evidence for a Coordination Number Change along the Lanthanide Series: FT-IR Investigation of the Solvates $[Ln(NO_3)_3(DMSO)_n]$ in Anhydrous Acetonitrile[1]

Jean-Claude G. Bünzli,* Jean-Pierre Metabanzoulou, Pascal Froidevaux, and Linpei Jin[2]

Received January 24, 1990

The interaction between lanthanide nitrates and dimethyl sulfoxide (DMSO) has been studied in anhydrous acetonitrile by FT-IR difference spectra. If $R = [DMSO]_t/[Ln(III)]_t$ is kept low enough (typically <9), nitrate ions do not dissociate and remain bonded in a bidentate fashion. A quantitative study of the ν_7(S-O) and ν_{22}(C-S) stretching modes has been performed for solutions generally 0.05 M in Ln(III), with Ln = La (0.012 M), Ce, Pr, Sm, Gd, Dy, Ho, Tm (0.029 M), Yb, and Lu, and R between 0 and 6. Average coordination numbers CN of the Ln(III) ions are reported for various compositions of the solutions. The data for $R = 6$, along with the previously published data for Nd, Eu, Tb, and Er, point to a large variation along the series, from 10.2 ± 0.3 for La to 8.4 ± 0.3 for Lu. La is 10-coordinate, and the main changes occur between Sm and Gd (0.6 unit) and between Er or Tm and Yb (0.6 unit). The coordination numbers depend upon the DMSO concentration, the data obtained for $R = 6$ being larger by approximately 0.5 unit than the coordination numbers determined for $R = 3$. Data for $R = 3$ confirm the CN change in the Pr-Eu region, but the variation is smaller; the small change between Gd and Lu occurs very gradually. For $R = 2$-6, there is an equilibrium between 9- and 10-coordinate species for the lighter lanthanides and between 8- and 9-coordinate species for the intermediate and heavier ions. Apparent stability constants have been calculated; they vary between $\log K_{10} = 2.2 \pm 0.1$ (La) to 0.9 ± 0.1 (Sm) and $\log K_9 = 1.8$ ● 0.1 (Eu) to 1.0 ± 0.1 (Lu).

Introduction

The 14 trivalent f-block ions, from Ce(III) to Lu(III), plus La(III), herein denoted Ln(III) ions, form an extended series of cations with the same formal charge and with similar chemical properties. The $4f^n5s^25p^6$ electronic configuration ensures that the bonding and stereochemistry of Ln(III) complexes and solvates are largely determined by both the predominantly ion-dipole bonding interaction between Ln(III) and the ligands and the steric repulsion between coordinated ligands. In fact, coordination numbers ranging from 3 to 14 have been reported in the solid state.[3,4] Many aspects of the coordination chemistry of these ions

(1) FT-IR and Fluorometric Investigation of Rare-Earth and Metal Ion Solvation. 9. Part 8: see ref 17.
(2) Present address: Department of Chemistry, Beijing Normal University, Beijing 100875, PRC.

(3) Jørgensen, C. K. In *Handbook on the Physics and Chemistry of Rare Earths*; Gschneidner, K. A., Jr., Eyring, L., Eds.; North-Holland: Amsterdam, 1979; Vol. 3, Chapter 23.

0020-1669/90/1329-3875$02.50/0